

# Construction of Metal–Organic Frameworks: Versatile Behaviour of a Ligand Containing Mono- and Bidentate Coordination Sites

Tia Jacobs and Michael J. Hardie\*<sup>[a]</sup>

**Abstract:** Five new coordination polymers based on a new 2,2'-bipyridine derived ligand *N,N'*-bis(pyridin-4-yl)-2,2'-bipyridine-5,5'-dicarboxamide (=L) are reported herein. Isostructural three-dimensional coordination polymers with a rare (4,6)-connected network of {4<sup>4</sup>.6<sup>2</sup>}.<sub>3</sub>{4<sup>6</sup>.8<sup>9</sup>}.<sub>2</sub> topology were synthesised from Cu(NO<sub>3</sub>)<sub>2</sub>, Zn(NO<sub>3</sub>)<sub>2</sub> or a

mixture of Cu(NO<sub>3</sub>)<sub>2</sub>/Fe(BF<sub>4</sub>)<sub>2</sub> with L in complexes  $\{[\text{Cu}_5\text{L}_6] \cdot (\text{NO}_3)_{10} \cdot (\text{H}_2\text{O})_{18}\}_\infty$  (**1**),  $\{[\text{Zn}_5\text{L}_6] \cdot (\text{NO}_3)_{10} \cdot (\text{H}_2\text{O})_{18}\}_\infty$  (**2**) and  $\{[\text{Fe}_x\text{Cu}_y\text{L}_6] \cdot (\text{NO}_3)_{10} \cdot (\text{H}_2\text{O})_{18}\}_\infty$  (**3**; where  $x + y = 5$ ). Complexes with two-dimensional grid structures resulted from treatment with CoCl<sub>2</sub> or Cd(NO<sub>3</sub>)<sub>2</sub> with L in complexes  $\{[\text{CoLCl}_2] \cdot \text{DMF}\}_\infty$  (**4**) and  $\{\text{CdL}(\text{NO}_3)_2\}_\infty$  (**5**).

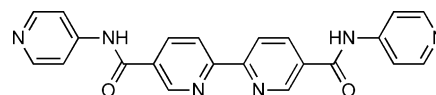
**Keywords:** 2,2'-bipyridine • (4,6)-connected topology • crystal structure • coordination polymers • metal–organic frameworks

## Introduction

The synthesis of coordination polymers has evoked an immense amount of recent interest.<sup>[1]</sup> The main focus has been on the construction of microporous coordination polymers due to their potential as gas storage materials,<sup>[2]</sup> nano-scale reaction vessels, and their catalytic<sup>[3]</sup> and magnetic properties.<sup>[4]</sup> It has become evident that judicious choice of metal centre and bridging ligand can afford infinite two- and three-dimensional networks that feature the desired characteristics and/or interesting structural topologies.<sup>[5]</sup> The potential of 4,4'-bipyridine as a rigid pillar (linear connecting ligand) in the construction of coordination polymers has long been realised and this ligand has seen widespread use as bridging ligand in the synthesis of two- and three-dimensional coordination polymers.<sup>[6]</sup> On the other hand, the use of 2,2'-bipyridine as chelating ligand as well as bridging ligand in the construction of three-dimensional coordination polymers have not been fully realised. Known examples stem from a few networks assembled from multicarboxy-2,2'-bipyridines, which exploit the anionic bis(carboxylato) moiety.<sup>[7,8]</sup> We, therefore, wanted to further investigate the potential of the 2,2'-bipyridine moiety as a building block for coordination polymers, firstly since the 2,2'-bipyridine metal trischelate structural node has an inherent diverging topology, and secondly since the 2,2'-bipyridine core could be decorated with a variety of pendant groups suitable for

secondary supramolecular interactions (specifically coordination).<sup>[9]</sup>

To this end we have been investigating the use of derivatives of 2,2'-bipyridine with additional monodentate coordination ability to prepare coordination polymers. ML<sub>3</sub> trischelate moieties can be coordinated further with additional pendant metal binding groups to afford two- or three-dimensional nets. While pursuing this design strategy towards the assembly of rigid coordination polymers for porous applications, we have synthesised five new framework complexes featuring the new ligand *N,N'*-bis(pyridin-4-yl)-2,2'-bipyridine-5,5'-dicarboxamide (=L). The frameworks are a



three-dimensional network  $\{[\text{M}_5\text{L}_6]\}_\infty$ , which could be self-assembled by using Cu(NO<sub>3</sub>)<sub>2</sub> (complex  $\{[\text{Cu}_5\text{L}_6] \cdot (\text{NO}_3)_{10} \cdot (\text{H}_2\text{O})_{18}\}_\infty$ , **1**), Zn(NO<sub>3</sub>)<sub>2</sub> (complex  $\{[\text{Zn}_5\text{L}_6] \cdot (\text{NO}_3)_{10} \cdot (\text{H}_2\text{O})_{18}\}_\infty$ , **2**) or a mixture of Fe(BF<sub>4</sub>)<sub>2</sub> and Cu(NO<sub>3</sub>) (complex  $\{[\text{Fe}_x\text{Cu}_y\text{L}_6] \cdot (\text{NO}_3)_{10} \cdot (\text{H}_2\text{O})_{18}\}_\infty$ , **3**); along with two closely related two-dimensional sheets in complexes  $\{[\text{CoLCl}_2] \cdot \text{DMF}\}_\infty$  (**4**) and  $\{\text{CdL}(\text{NO}_3)_2\}_\infty$  (**5**). The synthesis, crystal structures and behaviour of two of these frameworks towards guest solvent loss will be discussed, focusing on one example of each of the two topologies.

## Results and Discussion

**Synthesis and crystal structure of *N,N'*-bis(pyridin-4-yl)-2,2'-bipyridine-5,5'-dicarboxamide, L:** The ligand was synthesised in two steps from 5,5'-dimethyl-2,2'-bipyridine. By using

[a] Dr. T. Jacobs, Dr. M. J. Hardie  
School of Chemistry, University of Leeds  
Woodhouse Lane, Leeds, LS2 9JT (UK)  
Fax: (+44) 113 343-6565  
E-mail: m.j.hardie@leeds.ac.uk

Supporting information for this article is available on the WWW under <http://dx.doi.org/10.1002/chem.201101998>.

a literature procedure the 5,5'-dimethyl-2,2'-bipyridine can readily be oxidised to the 5,5'-dicarboxylic acid-2,2'-bipyridine with chromic acid ( $K_2Cr_2O_7$  in  $H_2SO_4$ ). Thereafter, the di-acid was converted to the acid chloride in situ with thionyl chloride, followed by treatment with 4-aminopyridine to afford L. The ligand was recrystallised from dimethyl sulfoxide (DMSO) to afford single crystals, the structures of which were elucidated by single-crystal X-ray diffraction in the triclinic space group,  $P\bar{1}$ . This revealed half of a ligand and one DMSO molecule per asymmetric unit. The bipyridine moiety of the ligand is co-planar with the nitrogen atoms in the *trans* positions. Each ligand hydrogen bonds to two DMSO molecules through N–H...O interactions ( $D\cdots A$ : 2.876(3) Å) between the amide and S=O moieties (Figure 1). The overall structure consists of the ternary hydrogen bonded units packing through edge-to-face  $\pi$  interactions. One interaction connects the ternary units along the stacking axis (crystallographic *b* axis; C...centroid 2.904 Å), while the second interaction connects neighbouring stacks (C...centroid 3.004 Å). Two more single crystal structures of the ligand have been obtained serendipitously from crystallisation trials, a hydrate, and pure ligand; these will not be

discussed here, but are shown in Figures S1 and S2 in the Supporting Information.

**Synthesis of 1–5:** Diffraction quality single-crystals of the networks were obtained from the treatment of L and the metal salts  $Cu(NO_3)_2$  (complex **1**),  $Zn(NO_3)_2$  (complex **2**),  $Fe(BF_4)_2/Cu(NO_3)_2$  (complex **3**),  $CoCl_2$  (complex **4**) and  $Cd(NO_3)_2$  (complex **5**). Complexes **1–4** were obtained from dimethylformamide solutions (in a 3:1 ligand-to-metal ratio) with diethyl ether as anti-solvent (network **4** crystallised without diethyl ether), while network **5** was afforded from an *N*-methyl-2-pyrrolidone solution, again with the slow diffusion of diethyl ether.

**Structure of  $\{[Cu_5L_6] \cdot (NO_3)_{10} \cdot (H_2O)_{18}\}_\infty$  (**1**):** The atomic numbering and connectivity of **1** are shown in Figure 2. The structure was solved and refined in the body centred cubic space group  $I432$ , and was shown to be a three-dimensional coordination polymer containing two distinct copper centres. Cu(1) is chelated by three bipyridine moieties in an octahedral coordination geometry resulting in delta ( $\Delta$ , right-handed) chirality ( $Cu(1)-N(1)=2.117(2)$  Å). All Cu(1) centres in the crystal structure have this chirality, which indicates that the trischelate enantiomers resolve spontaneously upon self-assembly into the three-dimensional network.<sup>[10]</sup> The bulk sample exists as a racemate. Cu(2) has octahedral geometry, with four monodentate *p*-pyridine moieties in square planar positions ( $Cu(2)-N(13)=2.011(2)$  Å). Two aqua ligands occupy the axial positions, one at  $Cu(2)-O(3)=2.310(4)$  Å, while the second water molecule forms a long interaction with Cu–O distance 2.760(5) Å.

If the unique copper centres are considered as nodes in the structure, the combination of the two copper coordination geometries thus afford a three-dimensional (4,6)-connected net. The connectivity as represented by the copper nodes is illustrated in Figure 3, and is composed of vertex-linked polyhedral prisms. Each of the stella octangula prisms has eight Cu(1) centres at its vertices, and three *fac*-4-pyridyl moieties emanate from each of these Cu(1) units to bind to a different symmetry-related square planar Cu(2) centre. Each Cu(2) is bound by four pyridyl groups from different Cu(1) nodes, to create a cube-like or stella octangula construction (Figure 3a and b). Each stella octangula is linked to eight others through its Cu(1) centres to create the vertex-linked network (Figure 3c). Other structural types involving coordination networks constructed from the metal-vertex-sharing of large polyhedral assemblies are known. For example, the vertex-linked  $M_6L_4$  octahedra from 2,4,6-tris(4-pyridyl)-1,3,5-triazine first reported as two interpenetrating nets by Robson et al.,<sup>[11a]</sup> and more recently the non-interpenetrated version reported by Fujita et al. by virtue of a change of metal centre.<sup>[11b]</sup> These two structures are also reminiscent of two other three-dimensional 3,4-connected networks, that is, a covalent organic framework (COF-108) described by Yaghi et al.,<sup>[11c]</sup> in which the octahedra are joined by shared vertices of tetrahedral carbons, and a metal-organic framework (MOF), HKUST-1, presented by

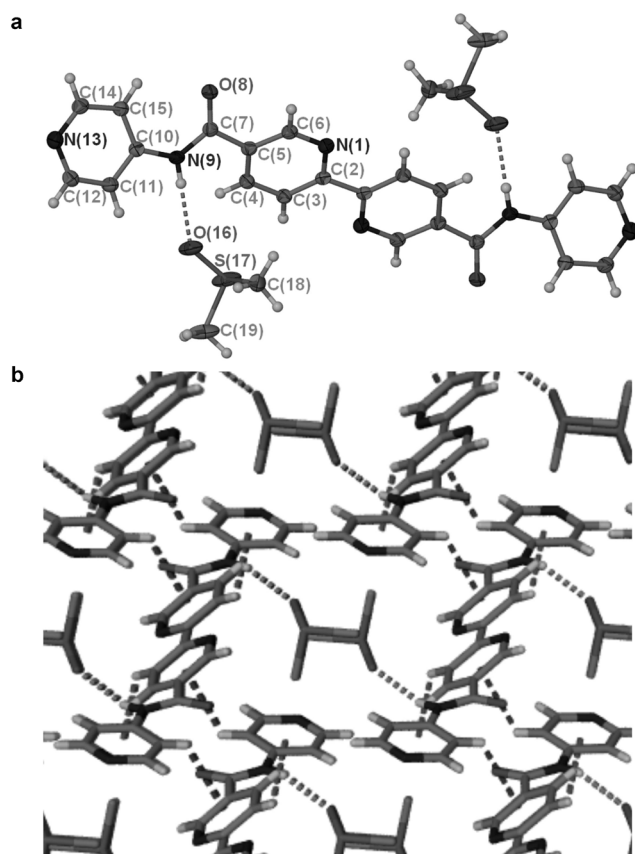


Figure 1. a) Ellipsoid plots (50% probability) of L·2DMSO, the asymmetric unit of the structure has been labelled. The N–H...O hydrogen bonds are shown as dashed lines. b) Stacking of the ternary hydrogen bonded unit shown along the crystallographic *b* axis. Two symmetry independent C–H... $\pi$  interactions are shown as well as one N–H...O interaction.

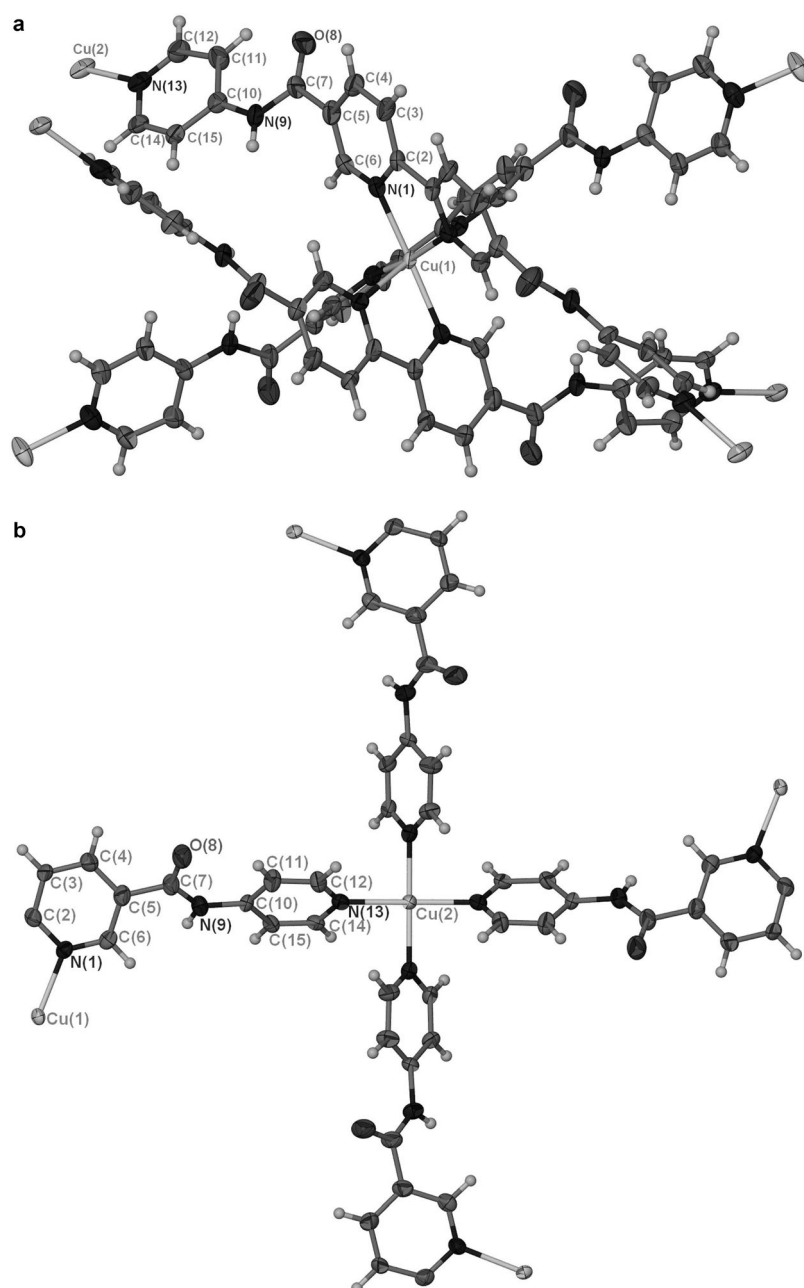


Figure 2. Ellipsoid plots showing: a) the octahedral coordination geometry around Cu(1), and b) the square planar coordination geometry of the monodentate *p*-pyridine moieties around Cu(2); only one half of the ligand as present in the asymmetric unit has been shown and the aqua ligands have been omitted for clarity.

Williams et al.,<sup>[11d]</sup> in which octahedra are joined by dicopper carboxylate paddlewheels. Polyhedra can also be linked into networks through other, non-vertex-sharing, mechanisms. For example, the metal–organic framework of truncated cuboctahedra linked by the use of tritopic ligands reported by Eddaoudi and colleagues,<sup>[11e]</sup> for a recent review on the subject see Zaworotko et al.<sup>[11f]</sup>

The Schläfli symbol for the network found in complex **2** is  $\{4^4 \cdot 6^2\}_3 \{4^6 \cdot 8^9\}_2$ , and the topological type, **soc**.<sup>[12]</sup> To the best of our knowledge this is a very rare topology in crystals, and has only been observed (classified) in a series of inorganic

clusters with cyanide bridging ligands<sup>[13a,b]</sup> as well as a porous MOF.<sup>[13c,d]</sup> In our structure no interpenetration is seen, and as a result of the cubic symmetry, three-dimensional intersecting channels are formed, as well as discrete solvent and anion-filled space within the prisms (Figure 4). The body diagonal Cu...Cu distance within the stella octangula prism is about 28.1 Å, which is also the diagonal Cu...Cu distance across each channel; hence the structure cannot interpenetrate, as a second network would not fit into the channels.

When water molecules are omitted the calculated guest-accessible free space is approximately 68% per unit cell, and the Cu(2)...Cu(2) distance (the width of the discrete cage) is 15.51 Å. Most of the nitrate anions (per  $\text{Cu}_{5/6}\text{L}(\text{NO}_3)_{5/3}$  formula unit) could be located in the electron density map, with one sixth of a nitrate missing from the asymmetric unit. Four water molecules could be modelled per formula unit, which correlates with elemental and thermal analysis of air-dried crystals; these showed that a total of three molecules of water are present per formula unit ( $\text{Cu}_{5/6}\text{L}_1(\text{NO}_3)_{5/3}$ ). This indicates the spontaneous loss of one water molecule. One of the nitrate anions in the asymmetric unit is seen to be encapsulated in the interstice between the three *fac* ligand arms, and accepts three hydrogen bonds from each of the N–H donors,

with  $\text{N}\cdots\text{O} = 2.943(3)$  Å (Figure 5). This phenomena has also been noted by Janiak et al., who found that metal trischelates of 5,5'-dicarbamate-2,2'-bipyridine show sulfate–anion binding in the pocket afforded by the three ligand arms.<sup>[14]</sup>

A further interesting point is the relative scarceness of structures reported to have been solved in the space group *I432*. Only four examples of supramolecular and MOF systems in this space group are known, these include a nanometer sized  $\text{M}_6\text{L}_8$  cage reported by Ueyama and co-workers, an isostructural MOF series based on  $\gamma$ -cyclodextrin by Stoddart and colleagues, a MOF based on a dicarboxylate

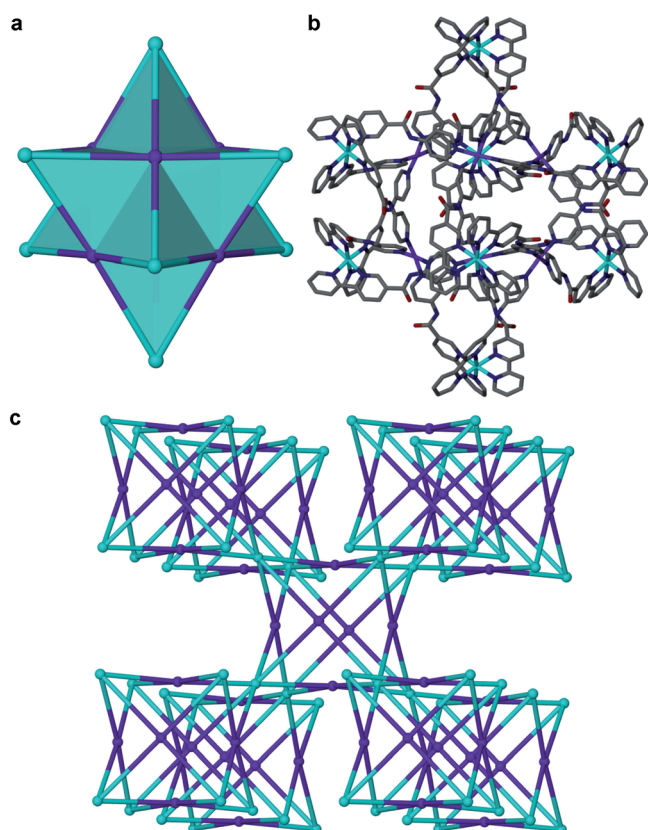


Figure 3. a) The stellated octahedron consisting of eight octahedral corners from Cu(1) centres (light blue) and six square planar Cu(2) sites (purple). b) The stellated octahedron as depicted in (a), presented in capped-stick and CPK colours (except for copper centres). On the Cu(1) corners, the parts of the ligand extending to the next octahedra have been omitted, hydrogen atoms have also been omitted. c) The Cu(1)⋯Cu(2) connectivity in the three-dimensional network of cubes, in which the blue nodes are the trischelate copper node, and the purple colour represents the square planar copper nodes. The body centred cubic framework is constructed from corner-sharing octahedral units.

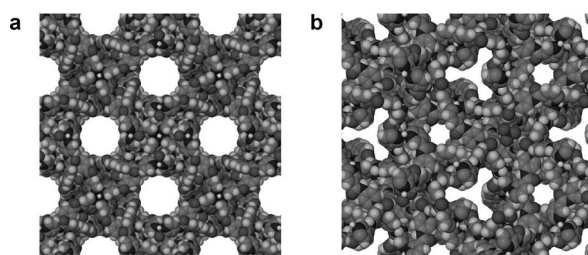


Figure 4. Space-filling diagrams of the network viewed along: a) [100] (equivalent views along [010] and [001]), and b) [111].

ligand by Jeong et al., as well as a hydrogen-bonded molecular assembly of calix[4]resorcinarenes.<sup>[15]</sup> There have also been a small number of reports of molecular complexes in this space group, for example, gallium and indium alkoxo-metalates and a hexanuclear nickel complex.<sup>[16]</sup>

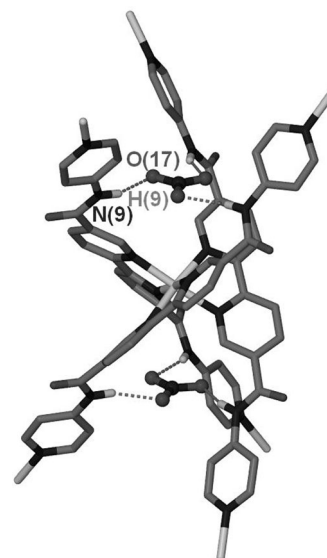


Figure 5. A depiction of the enclathrated nitrate anion in ball-and-stick representation and the trischelate shown in capped-stick representation, all hydrogen atoms not engaged in hydrogen bonding have been omitted.

#### Structures of $\{[\text{Zn}_x\text{L}_6] \cdot (\text{NO}_3)_{10} \cdot (\text{H}_2\text{O})_{18}\}_\infty$ (2) and $\{[\text{Fe}_x\text{Cu}_y\text{L}_6] \cdot (\text{NO}_3)_{10} \cdot (\text{H}_2\text{O})_{18}\}_\infty$ (3; where $x+y=5$ ):

These two networks are isostructural with **1** (see the Supporting Information for a short summary of relevant bond lengths). The existence of a mixture of iron and copper in network **3** was confirmed by energy-dispersive X-ray spectroscopy (EDX). Five crystals were randomly picked for analysis, and iron atomic percentages were semi-quantitatively determined to be in the range 6.60 to 32.93% with an average of 16.14% (if the sum of iron and copper is considered to be 100%) indicating a range of solid solutions are formed. Heterometallic coordination polymers are known and often involve a multitopic ligand approach in which “metallo-ligands” (coordination complexes) possess functional groups for further metal coordination.<sup>[17]</sup> The formation of heterometallic solid solutions of coordination polymers is rarer, but has been previously reported from solution crystallisations,<sup>[18a,b]</sup> as observed here, as well as from mechano-chemical synthesis.<sup>[18c]</sup>

**Structure of  $\{[\text{CoLCl}_2] \cdot \text{DMF}\}_\infty$  (4):** The atomic numbering and connectivity of **4** is shown in Figure 6a. The structure was determined to be in the monoclinic space group  $P2_1/c$ . One unique cobalt atom exists in an octahedral coordination environment (Figure 6b) with two chloride ligands (Co(1)–Cl(2) and Co(1)–Cl(3), 2.442(1) and 2.446(1) Å, respectively) and one chelating bipyridine moiety in the equatorial plane (Co(1)–N(1) and Co(1)–N(16), 2.188(2) and 2.217(2) Å, respectively).

Two 4-aminopyridine pendant groups occupy the remaining *trans* positions, with Co(1)–N(13)=2.216(2) Å and Co(1)–N(28)=2.239(2) Å. When the asymmetric unit of the network is considered, it is seen that the ligand is twisted, with one terminal 4-pyridyl moiety disordered over two po-

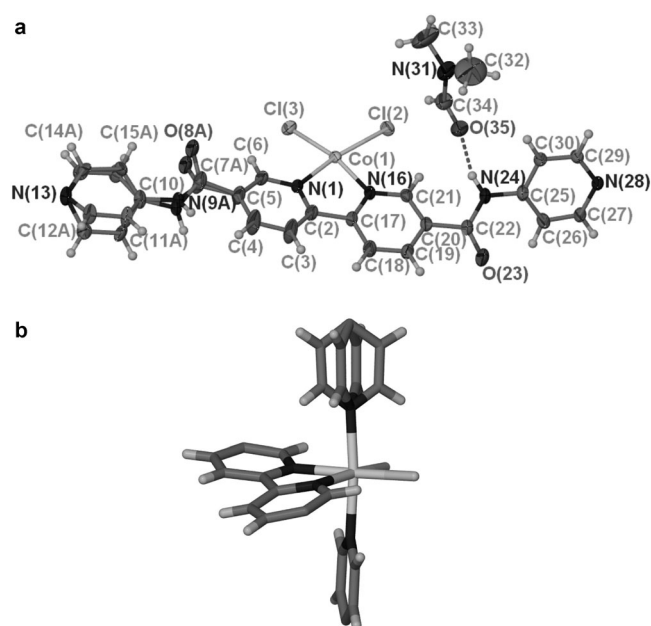


Figure 6. a) Asymmetric unit of **4** shown in an ellipsoid plot. b) A stick diagram showing the octahedral coordination geometry around Co(1), where the one 4-pyridyl arm is disordered over two positions.

sitions. The coordinated 2,2'-bipyridine moiety and *cis* chlorides are seen to occupy a slightly distorted square planar geometry around the cobalt. One DMF molecule could be located in the electron density map, and is seen to hydrogen bond via the C=O bond to the amide proton of the ligand ( $D\cdots A = 2.807(3) \text{ \AA}$ ).

The combination of the bridging nature of the ligand via its pendant 4-aminopyridine groups and the chelating nature of the 2,2'-bipyridine moiety results in an overall two-dimensional network (Figure 7a). The two-dimensional sheet is parallel to the (010) plane, and neighbouring sheets are related by inversion symmetry, creating an off-set packing arrangement along [100] (Figure 7b).

**Structure of  $\{CdL(NO_3)_2\}_\infty$  (**5**):** This structure was solved and elucidated in the space group  $P2_1$  and determined to be identical to **4** in terms of the two-dimensional sheet motif. The asymmetric unit is shown in Figure 8a, and once again the ligand is seen to be twisted with the one half of the bipyridine core displaying disorder. The metal centre is cadmium in this instance, and has as with **4**, an octahedral coordination environment consisting of a chelating bipyridine and two nitrate anions (one terminal and one chelating nitrate) in the equatorial positions, and two 4-aminopyridine moieties in the *trans* positions.

In this structure, the two-dimensional layers are parallel to the *bc* plane (Figure 9a) and stacked along the crystallographic *a* axis, whereas in **4** neighbouring layers were related by inversion symmetry (Figure 9b). This generates channels along the [100] direction and no solvent could be modelled in these channels from the electron density map.

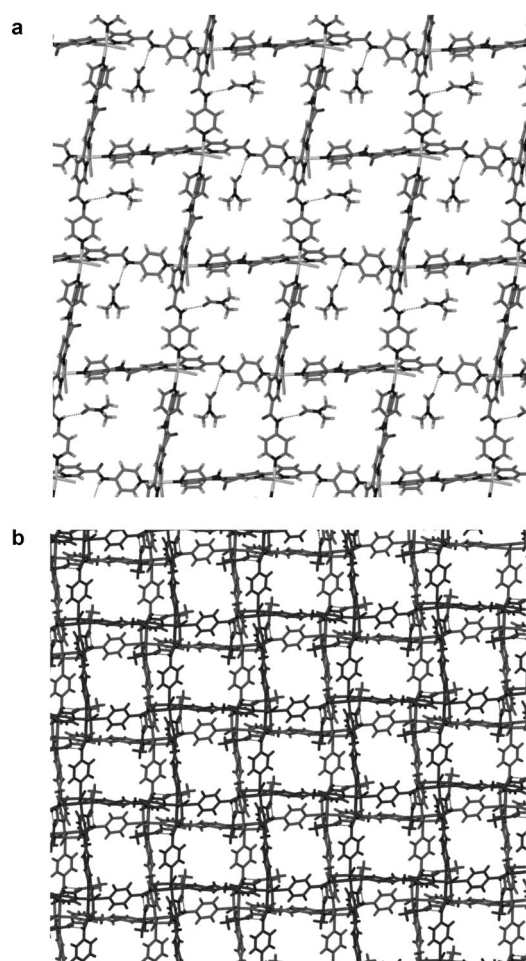


Figure 7. a) A diagram depicting the resulting two-dimensional network of **4**. b) The solvent-filled channels along [100] that result from the stacking of the two-dimensional networks.

**Degassing, thermal stability and powder diffraction of **1** and **4**:** As the five networks that were obtained in this study mainly have two topologies, we selected one example of each topology for further investigation. These were  $\{[Cu_5L_6] \cdot (NO_3)_{10} \cdot (H_2O)_{18}\}_\infty$  (**1**) and  $\{[CoLCl_2] \cdot DMF\}_\infty$  (**4**).

The bulk sample of **1** was subject to powder diffraction, and showed a good correlation with that of a powder trace simulated from the single-crystal structure (Figure 10b). Thermogravimetric analysis (TGA) of air-dried crystals of **1** only showed a small weight loss of about 9.5% up to 200 °C, shortly after which the material decomposed, with an onset temperature of 263.36 °C (Figure 10a). The 9.5% weight loss translates to approximately three molecules of water per formula unit ( $Cu_{5/6}L_1(NO_3)_{5/3}$ ), which is in agreement with the elemental analysis. We anticipate that no DMF molecules are present, since these would be expected to reside in the open channels of the structure, and could spontaneously desorb. From the crystal structure, we know, however, that several water molecules are present within the discrete volume inside the prism. Crystals of **1** were immersed in ethanol for two hours in an attempt to exchange the

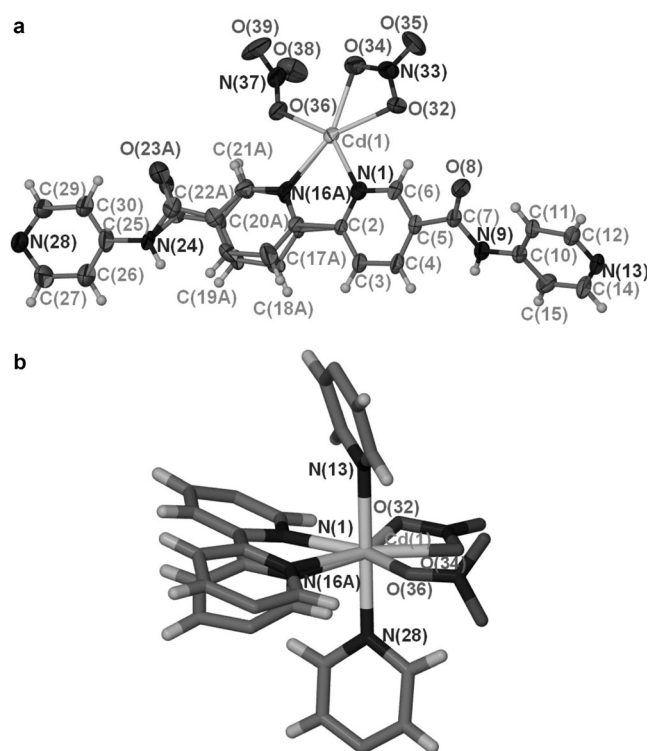


Figure 8. a) Asymmetric unit of **5** shown in an ellipsoid plot. b) A stick diagram showing the octahedral coordination geometry around Cd(1), where one of the pyridyl rings in the 2,2'-bipyridine core is disordered over two positions.

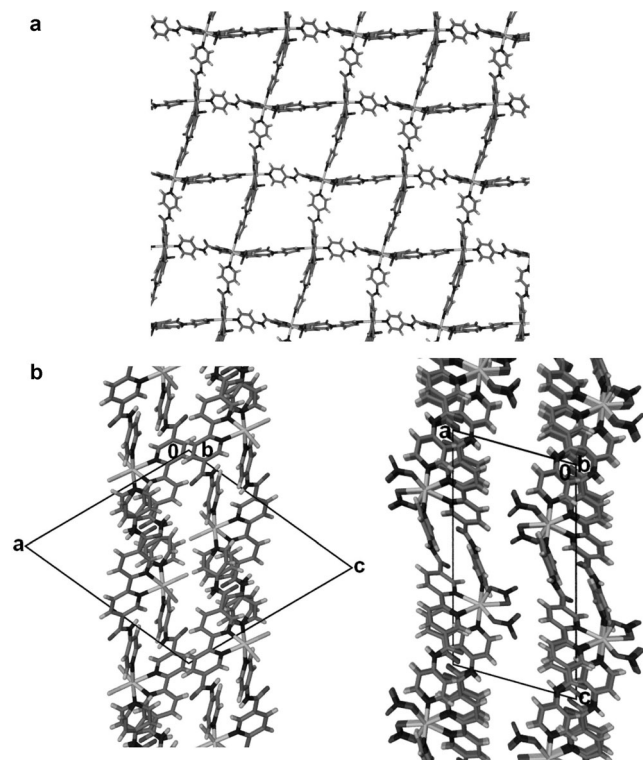


Figure 9. a) Stacking of the two-dimensional layers of **5** viewed along the stacking direction [100]. b) A comparison of **4** and **5**, as viewed along [010] for both structures.

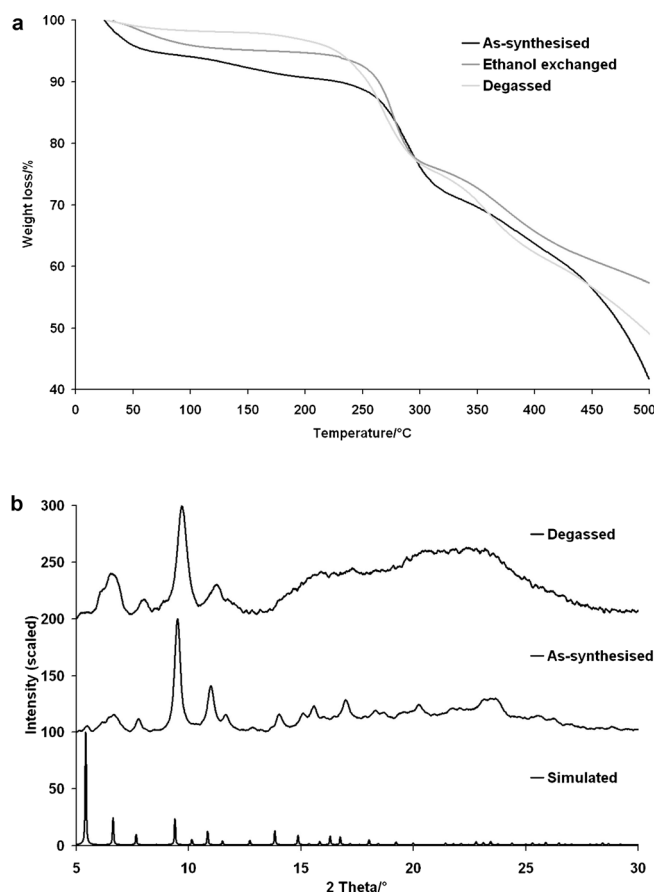


Figure 10. a) Thermal analysis, and b) powder diffraction data for **1**.

water molecules for ethanol molecules. The blue colour of the crystals remained unchanged during this solvent exchange and TGA showed a slightly reduced weight loss of 7.4%, which can be attributed to approximately 2.5 molecules of water or one molecule of ethanol per formula unit. Crystals of **1** were also subject to evacuation at 100°C for 3 days, which resulted in a dark green powder, and hereafter TGA showed a significantly reduced weight loss of about 3.4% (~1 molecule water). Powder diffraction data of the degassed material compares very well with the as-synthesised sample, however, with reduced crystallinity.

The bulk phase purity of **4** was determined to be homogeneous when powder diffractograms of the as-synthesised material were compared to a simulated diffractogram for the single-crystal structure (Figure 11b). TGA of air-dried crystals of **4** revealed that the loss of the DMF guest molecules occurs from room temperature, and the weight loss (~33.6%) corresponds to four molecules of DMF formula unit (CoCl<sub>2</sub>L). TGA and differential scanning calorimetry (DSC) also show that the material decomposes with an onset temperature of 395.75°C. Subsequently we attempted to desorb a sample of **4** by evacuating it for 3 days. Even though the sample changed from an orange to a green powder, TGA still showed a significant initial weight loss between 20 and 200°C (~20.6%) representing two mole-

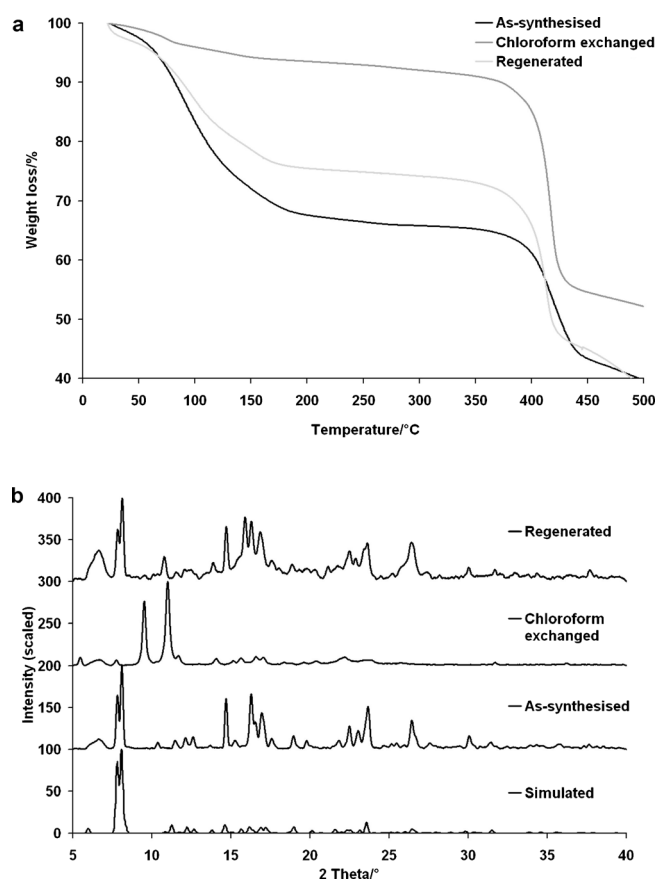


Figure 11. a) Thermal analysis, and b) powder diffraction data for **4**.

cules of DMF. The powder diffractogram of this evacuated material also showed good correlation with that of **4**. This material was then subjected to further evacuation at 60 °C for 7 days, TGA once again showed weight loss (~14.0%). At this point it was evident that very harsh conditions would have to be employed to completely rid the network of its DMF guests. A solvent-exchange strategy was then applied, and the as-synthesised material was soaked in chloroform for an hour. The TGA now obtained showed a much reduced weight loss of approximately 8% (TGA of chloroform-exchanged samples that were subject to evacuation, and heating under evacuation showed the same weight losses). From powder diffraction it can clearly be seen that this chloroform-exchanged material (orange-brown colour) exhibits a new phase; this can either be due to a scissoring of the two-dimensional square grid, or the movement of the two-dimensional layers relative to each other to form a non-porous staggered array (a combination of these two network rearrangements can also be envisaged). In a quick test to see if the DMF guest phase can be regenerated, the chloroform exchanged material was exposed to DMF vapour for a few days and then analysed by TGA and powder diffraction. The thermogram and diffractogram showed that DMF was indeed taken up again by the material, and these are shown along with the initial phase transformation from DMF-loaded to empty host phases in Figure 11 b. This network is,

therefore, capable of complete desorption and resorption of DMF guest molecules accompanied by a reversible phase change.

**Porosity of degassed phases:** Sorption studies were performed by probing the behaviour of these frameworks towards nitrogen at  $-196.15\text{ }^{\circ}\text{C}$  (liquid nitrogen) by using a ASAP2020 (accelerated surface area and porosimetry system). The porosity of **1** was investigated after the activation of the sample by immersing it in ethanol for 3 days. After this the material was further activated on the degas port of the gas sorption instrument at 80 °C for 20 h. The sorption experiment was immediately carried out, and showed that the sample was not porous to nitrogen (Figure 12). Compound **4** was activated by evacuation at 200 °C for 4 h prior to gas sorption studies. The obtained sorption isotherms showed that the sample is not permeable to nitrogen, with the rise in sorption near saturation pressure due to capillary condensation in the sample.

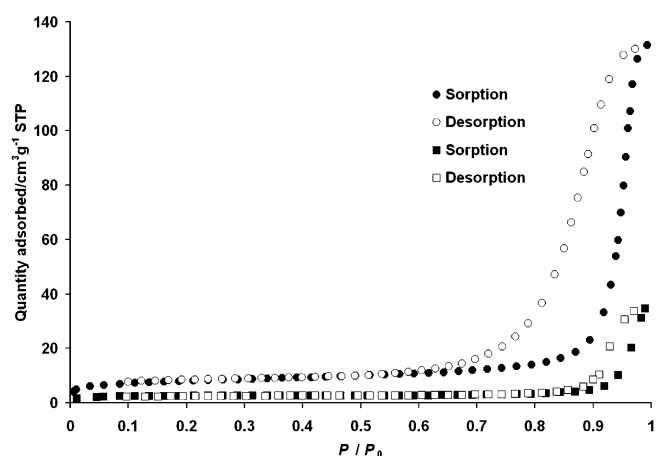


Figure 12. Sorption and desorption of samples of **1** (●) and **4** (■) degassed with heating.

## Conclusion

The new ligand *N,N'*-bis(pyridin-4-yl)-2,2'-bipyridine-5,5'-dicarboxamide (**L**) features both chelating and monodentate metal-binding sites. Trischelate and monochelate metal complexes of **L** have been shown to be effective structural nodes for the construction of three- or two-dimensional coordination polymer materials. The three-dimensional structure has a highly unusual  $\{4^4 \cdot 6^2\}_3\{4^6 \cdot 8^9\}_2$  or **soc** topology type, which can also be described as vertex-sharing stella octangula prisms. It is a structure that cannot interpenetrate, thus maximising cavities and channels, and features both orthogonal nano-sized channels and large internal cavities of the prisms. Grid-like two-dimensional coordination polymers are formed from monochelate complexes and these show reversible dynamic behaviour on solvent exchange. The use of simple 2,2'-bipyridine chelate complexes with additional metal binding sites on the ligands as structural nodes or

building units for coordination polymers remains relatively unexplored. These materials illustrate that this is an alternative approach to generating new potentially porous materials, and this is the subject of ongoing work.

## Experimental Section

**General:** IR spectra were measured for compounds as solid-state samples on a Perkin–Elmer FTIR spectrometer. Elemental analyses were performed at the micro-analytical laboratory at the University of Leeds. ESMS were recorded by using Micromass LCT or Bruker MicroTOFFocus mass spectrometers. NMR spectra were recorded on Bruker Avance 500 MHz spectrometer by using 5 mm probes. The  $^1\text{H}$  NMR spectrum was referenced relative to the solvent peak:  $[\text{D}_6]\text{DMSO}$ ,  $\delta = 2.6$  ppm. Simultaneous thermogravimetric analysis and differential scanning calorimetry were carried out on a TA instruments SDT Q600 by using a  $5^\circ\text{Cmin}^{-1}$  heating rate under a nitrogen atmosphere with a  $50\text{ mLmin}^{-1}$  flow rate. Volumetric sorption was carried out on a Micromeritics ASAP 2020 instrument. X-ray powder diffraction experiments were carried out on a Bruker D8 instrument by using  $\text{Cu-K}\alpha$  radiation ( $\lambda = 1.5418\text{ \AA}$ ). EDX was performed on a Jeol JSM-6610 LV instrument, coupled to an INCA EDS system. Unless otherwise stated, reagents were obtained from commercial sources and used as received. 2,2'-bipyridine-5,5'-dicarboxylic acid was prepared according to a literature procedure.<sup>[19]</sup>

**Synthesis of L (*N,N'*-bis(pyridin-4-yl)-2,2'-bipyridine-5,5'-dicarboxamide):** 2,2'-Bipyridine-5,5'-dicarboxylic acid (450 mg, 1.84 mmol) was activated by reflux in thionyl chloride (10 mL) until the solution was clear. The thionyl chloride was removed in situ and the acid chloride was suspended in dry dichloromethane (~80 mL) and brought to reflux under argon. In a second flask 4-aminopyridine (432.9 mg, 4.60 mmol) was dissolved in dry dichloromethane (~30 mL) and dry triethylamine (2.56 mL, 18.40 mmol) was added. The mixture was added dropwise via cannula to the acid chloride solution while under reflux. Upon complete addition of the mixture, heating at reflux was continued for a further 30 min, and allowed to cool to room temperature, overnight, with continuous stirring. The light yellow solid was removed by filtration, washed with dichloromethane, water and finally diethyl ether to afford a light yellow coloured powder. Inspection of the  $^1\text{H}$  NMR spectrum of the solid revealed a single compound, therefore, further purification was not performed. However, the material can be further purified by recrystallisation from a hot dimethylformamide solution to afford a white-creamy crystalline solid; yield: 88%; m.p. > 360°C;  $^1\text{H}$  NMR (500 MHz,  $[\text{D}_6]\text{DMSO}$ , 25°C):  $\delta = 7.80$  (dd,  $^3J(\text{H,H}) = 4.8$  and  $^4J(\text{H,H}) = 1.68$  Hz, 4H; NCHCH), 8.525–8.538, (m, 6H; NCHCH and NCCHCH), 8.633 (d,  $^3J(\text{H,H}) = 8.2$  Hz, 2H; NCCH), 9.266 (d,  $^4J(\text{H,H}) = 2.3$  Hz, 2H; NCHC), 10.884 ppm (s, 2H; NH); IR (ATR):  $\tilde{\nu} = 3361$  (s), 1900 (m), 1739 (w), 1667 (brs), 1591 (brs), 1415 (s), 1295 (brs), 1114 (s), 1025 (s), 991 (s), 896 (s), 855 (s), 821 (s), 758 (s), 724  $\text{cm}^{-1}$  (s); MS (ESI+):  $m/z$  (%): 397.14 (100)  $[\text{M} + \text{H}^+]$ , 199.08 (24)  $[\text{M} + 2\text{H}^+]$ ; HRMS-ToF (ESI+): found: 397.1416  $[\text{M} + \text{H}^+]$ , calcd for  $\text{C}_{22}\text{H}_{17}\text{N}_6\text{O}_2$  397.1408; elemental analysis calcd (%) for  $\text{C}_{22}\text{H}_{16}\text{N}_6\text{O}_2 \cdot 1/4\text{H}_2\text{O}$ : C 65.91, H 4.15, N, 20.96; found: C 66.10, H 4.10, N 20.95.

### Synthesis of complexes

**Synthesis of 1:** For single-crystal diffraction (SCD):  $\text{Cu}(\text{NO}_3)_2 \cdot 2/2\text{H}_2\text{O}$  (0.5 mg, 0.002 mmol) was dissolved in DMF (0.2 mL) and added to a solution of L (2.4 mg, 0.006 mmol) in DMF (1 mL). The vial with DMF solution was placed in a bigger vial containing diethyl ether. After one week blue-purple octahedral crystals formed.

**Bulk sample:** L (118.9 mg, 0.3 mmol) was dissolved in DMF (30 mL) by slight stirring and stirring, a solution of  $\text{Cu}(\text{NO}_3)_2 \cdot 6\text{H}_2\text{O}$  (72.8 mg, 0.3 mmol) in DMF (5 mL) was added to the stirring solution. The green solution was allowed to cool to room temperature and after a few days the solution is a dark green suspension with blue solid. The green suspension was decanted from the blue solid, and the blue crystals further rinsed with DMF to remove the last traces of green material. The blue

crystals were then rinsed with a small amount of ethanol and allowed to air dry. After being air-dried 65 mg was obtained, this translates to 36% yield if a molecular formula of  $[\text{Cu}_{5/6}(\text{NO}_3)_{5/3}](\text{H}_2\text{O})_3$  is considered (as determined from thermogravimetric analysis). An air-dried sample was submitted for elemental analysis. IR (ATR):  $\tilde{\nu} = 3271$  (brs), 1699 (s), 1594 (s), 1514 (s), 1476 (m), 1423 (s), 1332 (s), 1213 (s), 1126 (s), 1014 (s), 898 (s), 829 (s), 755  $\text{cm}^{-1}$  (s); elemental analysis calcd (%) for  $\text{Cu}_{5/6}(\text{NO}_3)_{5/3} \cdot \text{C}_{22}\text{H}_{16}\text{N}_6\text{O}_2 \cdot 3\text{H}_2\text{O}$ : C 43.55, H 3.65, N 17.70; found: C 43.90, H 3.45, N 17.45.

**Synthesis of 2:**  $\text{Zn}(\text{NO}_3)_2 \cdot 6\text{H}_2\text{O}$  (0.6 mg, 0.002 mmol) was dissolved in DMF (0.2 mL) and added to a solution of L (2.4 mg, 0.006 mmol) in DMF (1 mL). Diisopropyl ether was diffused into this solution to afford colourless block-shaped crystals; yield: 32%. A sample for elemental analysis was dried under vacuum at 100°C for 15 h. IR (ATR):  $\tilde{\nu} = 3182$  (brm), 1588 (s), 1289 (s), 1210 (s), 1123 (s), 1039 (s), 899 (s), 831  $\text{cm}^{-1}$  (s); elemental analysis calcd (%) for  $\text{Zn}_{5/6}(\text{NO}_3)_{5/3} \cdot \text{C}_{22}\text{H}_{16}\text{N}_6\text{O}_2 \cdot 2/3\text{H}_2\text{O} \cdot 2/3\text{C}_3\text{H}_7\text{NO}$ : C 46.87, H 3.61, N 18.98; found: C 47.20, H 3.70, N 18.10.

**Synthesis of 3:** L (1.2 mg, 0.003 mmol) was dissolved in DMF (1 mL) and  $\text{Fe}(\text{BF}_4)_2 \cdot 6\text{H}_2\text{O}$  (0.3 mg, 0.001 mmol) in DMF (0.05 mL) was added followed by  $\text{Cu}(\text{NO}_3)_2 \cdot 2/2\text{H}_2\text{O}$  (0.3 mg, 0.0015 mmol) in DMF (0.25 mL). After a few weeks grey crystals were formed; yield: 30%. A sample for elemental analysis was dried under vacuum at 150°C for 15 h. IR (ATR):  $\tilde{\nu} = 3383$  (brs), 1652 (s), 1601 (s), 1514 (s), 1478 (s), 1334 (s), 1212 (s), 1126 (s), 1031 (s), 900 (s), 838  $\text{cm}^{-1}$  (s); elemental analysis calcd (%) for  $\text{Fe}_{1/12}\text{Cu}_{3/4}(\text{NO}_3)_{5/3} \cdot \text{C}_{22}\text{H}_{16}\text{N}_6\text{O}_2 \cdot 3/2\text{H}_2\text{O}$ : C 45.63, H 3.31, N 18.54; found: C 45.75, H 3.40, N 17.35.

**Synthesis of 4:** For SCD a solution of  $\text{CoCl}_2 \cdot 6\text{H}_2\text{O}$  (0.5 mg, 0.002 mmol) and L (2.4 mg, 0.006 mmol) in DMF (1 mL) was diffused with diethyl ether, red crystals were obtained after 5 days.

**Bulk sample:** The synthesis of 4 was easily scaled-up from the crystallisation. L (118.9 mg, 0.3 mmol) was dissolved in DMF (30 mL) by gently heating the stirred solution and a solution of  $\text{CoCl}_2 \cdot 6\text{H}_2\text{O}$  (71.4 mg, 0.3 mmol) in DMF (5 mL) was added slowly. The clear dark green solution was then allowed to cool to room temperature and after a few days the orange-red solid that formed was removed by filtration, washed with DMF and a small volume of ethanol was added to yield an orange-brown powder. After being air-dried 190 mg was obtained, this translates to 78% yield if a molecular formula of  $\text{CoCl}_2 \cdot 4\text{DMF}$  is considered (as determined from thermogravimetric analysis). A sample for elemental analysis was dried at 70°C for 30 h. IR (ATR):  $\tilde{\nu} = 3262$  (brs), 1698 (s), 1596 (s), 1508 (s), 1213 (m), 1125 (s), 1031 (s), 899 (s), 828 (s), 752  $\text{cm}^{-1}$  (s); elemental analysis calcd (%) for  $\text{CoCl}_2 \cdot 2\text{C}_{22}\text{H}_{16}\text{N}_6\text{O}_2 \cdot 2/2\text{H}_2\text{O}$ : C 46.25, H 3.71, N, 14.71; found: C 46.45, H 3.50, N 14.70.

**Synthesis of 5:**  $\text{Cd}(\text{NO}_3)_2 \cdot 4\text{H}_2\text{O}$  (0.6 mg, 0.002 mmol) was dissolved in *N*-methyl-2-pyrrolidone (NMP; 0.2 mL) and added to a solution of L (2.4 mg, 0.006 mmol) in NMP (1 mL). The solution was placed in a bigger vial containing diethyl ether, and irregular colourless blocks were visible after a few weeks (crystals could also be obtained from DMF with diethyl ether diffusion); yield: 37%. A sample for elemental analysis was dried at 100°C for 15 h. Elemental analysis calcd (%) for  $\text{C}_{22}\text{H}_{16}\text{N}_6\text{CdO}_8 \cdot 1/4\text{C}_2\text{H}_5\text{NO}$ : C 42.46, H 3.00, N 17.35; found: C 42.46, H 2.80, N 17.57; IR (ATR):  $\tilde{\nu} = 3359$  (brs), 1664 (s), 1599 (s), 1509 (s), 1425 (s), 1334 (s), 1298 (s), 1212 (m), 1127 (m), 1032 (m), 899 (m), 830 (m), 754  $\text{cm}^{-1}$  (m).

**Crystal structure determinations:** Crystals were attached to the end of a MiTeGen mount by using paratone oil. X-ray data were collected with  $\text{MoK}\alpha$  radiation ( $\lambda = 0.71073\text{ \AA}$ ) on a Bruker Nonius X8 diffractometer fitted with an Apex II detector, FR591 rotating anode operating at 4 kW and an Oxford cryosystems cryostream plus cooling system. Data reduction was carried out by means of a standard procedure by using the Apex2 software package. When necessary, empirical corrections were performed by using SADABS. Structures were either solved by direct methods or Patterson methods by using SHELXS<sup>[20]</sup> or SIR-2004<sup>[21]</sup> and refined by fullmatrix least-squares on  $F^2$  by SHELXL<sup>[20]</sup> interfaced through the program X-Seed.<sup>[22]</sup> In general, all non-hydrogen atoms were refined anisotropically and hydrogen atoms were included as invariants at geometrically estimated positions. Diagrams were generated by using

the program X-Seed<sup>[22]</sup> as an interface to POV-Ray.<sup>[23]</sup> CCDC 829646 (**1**), 829647 (**2**), 829648 (**3**), 829649 (**4**), 829650 (**5**), 829651 (L·2DMSO), 829652 (L), 829653 (L·2H<sub>2</sub>O) contain the supplementary crystallographic data for this paper. These data can be obtained free of charge from The Cambridge Crystallographic Data Centre via [www.ccdc.cam.ac.uk/data\\_request/cif](http://www.ccdc.cam.ac.uk/data_request/cif).

All crystals lost solvent quickly and turned opaque upon removal from the mother liquor. In the case of structures **1–3** the crystal system was determined as cubic with body centring and there are six possible space groups that all have equivalent reflection conditions. A systematic look at the solutions produced by SIR-2004 for all of these six space groups finally yielded the best solution in the chiral space group *I*432. From EDX measurements it was determined that different crystals of **3** contained different ratios of Fe-to-Cu. However, it was not possible to determine the Fe-to-Cu ratio in the crystal used for the collection of X-ray diffraction data, and therefore, the occupancy assignment that afforded the best *U*<sub>iso</sub> and *R*1 values were assumed to be correct (this reflected a 3:2 ratio of Cu/Fe). The diffraction data of the crystal of **5** showed signs of pseudo-merohedral twinning, and could be successfully refined after two twin laws were included in the refinement. The contributions from disordered solvent molecules (and anions in the case of **1–3**) were removed by the SQUEEZE<sup>[24]</sup> routine within PLATON<sup>[25]</sup> and the outputs from the SQUEEZE calculations are attached to each CIF file.

**Crystal data for L·2DMSO:** C<sub>26</sub>H<sub>28</sub>N<sub>6</sub>O<sub>4</sub>S<sub>2</sub>, *M* = 552.66, colourless rod, 0.30 × 0.13 × 0.09 mm<sup>3</sup>, triclinic, space group *P*1̄ (No. 2), *a* = 7.5178(8), *b* = 8.6729(9), *c* = 10.6312(11) Å, *α* = 80.574(7), *β* = 79.588(6), *γ* = 84.448(6)°, *V* = 670.93(12) Å<sup>3</sup>, *Z* = 1, *ρ*<sub>calcd</sub> = 1.368 g cm<sup>-3</sup>, *F*<sub>000</sub> = 290, MoK<sub>α</sub> radiation, *λ* = 0.71073 Å, *T* = 150(2) K, 2*θ*<sub>max</sub> = 52.9°, 10188 reflections collected, 2726 unique (*R*<sub>int</sub> = 0.0381). Final GooF = 1.042, *R*1 = 0.0666, *wR*2 = 0.1466, *R* indices based on 2191 reflections with *I* > 2σ(*I*) (refinement on *F*<sup>2</sup>), 172 parameters, 0 restraints. Lorentz polarisation and absorption corrections applied, *μ* = 0.243 mm<sup>-1</sup>.

**Crystal data for 1:** C<sub>132</sub>H<sub>144</sub>Cu<sub>5</sub>N<sub>46</sub>O<sub>66</sub>, *M* = 3748.63, purple octahedron, 0.20 × 0.20 × 0.20 mm<sup>3</sup>, cubic, space group *I*432 (No. 211), *a* = 32.452(2) Å, *V* = 34176(4) Å<sup>3</sup>, *Z* = 4, *ρ*<sub>calcd</sub> = 0.729 g cm<sup>-3</sup>, *F*<sub>000</sub> = 7724, MoK<sub>α</sub> radiation, *λ* = 0.71073 Å, *T* = 30(2) K, 2*θ*<sub>max</sub> = 52.8°, 90317 reflections collected, 5860 unique (*R*<sub>int</sub> = 0.0504). Final GooF = 1.019, *R*1 = 0.0503, *wR*2 = 0.1358, *R* indices based on 4651 reflections with *I* > 2σ(*I*) (refinement on *F*<sup>2</sup>), 189 parameters, 2 restraints. Lorentz polarisation and absorption corrections applied, *μ* = 0.358 mm<sup>-1</sup>. Absolute structure parameter = 0.070(18).<sup>[26]</sup>

**Crystal data for 2:** C<sub>132</sub>H<sub>132</sub>N<sub>46</sub>O<sub>60</sub>Zn<sub>5</sub>, *M* = 3649.69, yellow pyramid, 0.27 × 0.20 × 0.13 mm<sup>3</sup>, cubic, space group *I*432 (No. 211), *a* = 33.0880(12) Å, *V* = 36225(2) Å<sup>3</sup>, *Z* = 4, *ρ*<sub>calcd</sub> = 0.669 g cm<sup>-3</sup>, *F*<sub>000</sub> = 7504, MoK<sub>α</sub> radiation, *λ* = 0.71073 Å, *T* = 173(2) K, 2*θ*<sub>max</sub> = 44.0°, 91583 reflections collected, 3727 unique (*R*<sub>int</sub> = 0.0517). Final GooF = 1.055, *R*1 = 0.0525, *wR*2 = 0.1435, *R* indices based on 3068 reflections with *I* > 2σ(*I*) (refinement on *F*<sup>2</sup>), 198 parameters, 5 restraints. Lorentz polarisation and absorption corrections applied, *μ* = 0.373 mm<sup>-1</sup>. Absolute structure parameter = 0.04(2).<sup>[26]</sup>

**Crystal data for 3:** C<sub>132</sub>H<sub>108</sub>Cu<sub>3</sub>Fe<sub>2</sub>N<sub>46</sub>O<sub>48</sub>, *M* = 3396.87, grey hexagon, 0.17 × 0.14 × 0.01 mm<sup>3</sup>, cubic, space group *I*432 (No. 211), *a* = 32.637(4), *V* = 34764(6) Å<sup>3</sup>, *Z* = 4, *ρ*<sub>calcd</sub> = 0.631 g cm<sup>-3</sup>, *F*<sub>000</sub> = 6740, MoK<sub>α</sub> radiation, *λ* = 0.71073 Å, *T* = 250(2) K, 2*θ*<sub>max</sub> = 47.8°, 55401 reflections collected, 4522 unique (*R*<sub>int</sub> = 0.0370). Final GooF = 1.003, *R*1 = 0.0390, *wR*2 = 0.1102, *R* indices based on 3739 reflections with *I* > 2σ(*I*) (refinement on *F*<sup>2</sup>), 161 parameters, 0 restraints. Lorentz polarisation and absorption corrections applied, *μ* = 0.303 mm<sup>-1</sup>. Absolute structure parameter = 0.039(19).<sup>[26]</sup>

**Crystal data for 4:** C<sub>25</sub>H<sub>23</sub>Cl<sub>2</sub>CoN<sub>7</sub>O<sub>3</sub>, *M* = 599.33, orange block, 0.11 × 0.10 × 0.09 mm<sup>3</sup>, monoclinic, space group *P*2<sub>1</sub>/*c* (No. 14), *a* = 16.1896(15), *b* = 16.3056(14), *c* = 17.2037(14) Å, *β* = 113.868(4)°, *V* = 4153.1(6) Å<sup>3</sup>, *Z* = 4, *ρ*<sub>calcd</sub> = 0.959 g cm<sup>-3</sup>, *F*<sub>000</sub> = 1228, MoK<sub>α</sub> radiation, *λ* = 0.71073 Å, *T* = 150(2) K, 2*θ*<sub>max</sub> = 49.5°, 39475 reflections collected, 7074 unique (*R*<sub>int</sub> = 0.0567). Final GooF = 1.038, *R*1 = 0.0411, *wR*2 = 0.1024, *R* indices based on 5110 reflections with *I* > 2σ(*I*) (refinement on *F*<sup>2</sup>), 383 parameters, 8 restraints. Lorentz polarisation and absorption corrections applied, *μ* = 0.569 mm<sup>-1</sup>.

**Crystal data for 5:** C<sub>22</sub>H<sub>16</sub>CdN<sub>8</sub>O<sub>8</sub>, *M* = 632.83, colourless block, 0.30 × 0.25 × 0.15 mm<sup>3</sup>, monoclinic, space group *P*2<sub>1</sub> (No. 4), *a* = 10.3790(6), *b* =

14.9220(10), *c* = 19.0290(13) Å, *β* = 105.7710(10)°, *V* = 2836.2(3) Å<sup>3</sup>, *Z* = 2, *ρ*<sub>calcd</sub> = 0.741 g cm<sup>-3</sup>, *F*<sub>000</sub> = 632, MoK<sub>α</sub> radiation, *λ* = 0.71073 Å, *T* = 150(2) K, 2*θ*<sub>max</sub> = 54.2°, 12321 reflections collected, 8333 unique (*R*<sub>int</sub> = 0.0293). Final GooF = 0.805, *R*1 = 0.0349, *wR*2 = 0.0728, *R* indices based on 6479 reflections with *I* > 2σ(*I*) (refinement on *F*<sup>2</sup>), 428 parameters, 604 restraints. Lorentz polarisation and absorption corrections applied, *μ* = 0.413 mm<sup>-1</sup>. Absolute structure parameter = 0.22(2).<sup>[26]</sup>

## Acknowledgements

We thank Benjamin Murray and Tamsin Malkin for use of powder diffractometer; Fiona Meldrum and Alexander Kulak for use of thermal analysis and sorption facilities; Algy Kazlaucinas for EDX measurements; and the Leverhulme Trust for funding.

- a) B. F. Abrahams, B. F. Hoskins, D. M. Michail, R. Robson, *Nature* **1994**, *369*, 727–729; b) S. R. Batten, R. Robson, *Angew. Chem.* **1998**, *110*, 1558–1595; *Angew. Chem. Int. Ed.* **1998**, *37*, 1460–1494; c) A. J. Blake, N. R. Champness, P. Hubberstey, W. S. Li, M. A. Withersby, M. Schroder, *Coord. Chem. Rev.* **1999**, *183*, 117–138; d) R. Robson, *J. Chem. Soc. Dalton Trans.* **2000**, 3735–3744; e) B. Moulton, M. J. Zaworotko, *Chem. Rev.* **2001**, *101*, 1629–1658; f) L. Brammer, *Chem. Soc. Rev.* **2004**, *33*, 476–489.
- a) S. L. James, *Chem. Soc. Rev.* **2003**, *32*, 276–288; b) M. Eddaoudi, J. Kim, N. Rosi, D. Vodak, J. Wachter, M. O’Keefe, O. M. Yaghi, *Science* **2002**, *295*, 469–472; c) H. K. Chae, D. Y. Siberio-Perez, J. Kim, Y. Go, M. Eddaoudi, A. J. Matzger, M. O’Keefe, O. M. Yaghi, *Nature* **2004**, *427*, 523–527; d) J. L. C. Rowsell, A. R. Millward, K. S. Park, O. M. Yaghi, *J. Am. Chem. Soc.* **2004**, *126*, 5666–5667; e) D. Bradshaw, J. B. Claridge, E. J. Cussen, T. J. Prior, M. J. Rosseinsky, *Acc. Chem. Res.* **2005**, *38*, 273–282; f) J. L. C. Rowsell, O. M. Yaghi, *Angew. Chem. Int. Ed.* **2005**, *44*, 4670–4679; g) A. R. Millward, O. M. Yaghi, *J. Am. Chem. Soc.* **2005**, *127*, 17998–17999.
- a) J. S. Seo, D. Whang, H. Lee, S. I. Jun, J. Oh, Y. J. Jeon, K. Kim, *Nature* **2000**, *404*, 982–986; b) B. Kesanli, W. B. Lin, *Coord. Chem. Rev.* **2003**, *246*, 305–326.
- a) C. Janiak, *Dalton Trans.* **2003**, 2781–2804; A. Y. Robin, K. M. Fromm, *Coord. Chem. Rev.* **2006**, *250*, 2127–2157; b) O. Kahn, C. J. Martinez, *Science* **1998**, *279*, 44–48; c) O. Kahn, *Acc. Chem. Res.* **2000**, *33*, 647–657.
- R. Robson, *Dalton Trans.* **2008**, 5113–5131.
- a) M. Kondo, T. Okubo, A. Asami, S.-i. Noro, T. Yoshitomi, S. Kitagawa, T. Ishii, H. Matsuzaka, K. Seki, *Angew. Chem.* **1999**, *111*, 190–193; *Angew. Chem. Int. Ed.* **1999**, *38*, 140–143; b) H. Chun, D. N. Dytsev, H. Kim, K. Kim, *Chem. Eur. J.* **2005**, *11*, 3521–3529; c) C. Gao, S. Liu, L. Xie, Y. Ren, J. Cao, C. Sun, *CrystEngComm* **2007**, *9*, 545–547; d) L.-F. Ma, L.-Y. Wang, X.-K. Huo, Y.-Y. Wang, Y.-T. Fan, J.-G. Wang, S.-H. Chen, *Cryst. Growth Des.* **2008**, *8*, 620–628; e) L. Carlucci, G. Ciani, D. M. Proserpio, A. Sironi, *J. Chem. Soc. Chem. Commun.* **1994**, 2755–2756; f) L. R. Macgillivray, S. Subramanian, M. J. Zaworotko, *J. Chem. Soc. Chem. Commun.* **1994**, 1325–1326; g) O. M. Yaghi, G. M. Li, *Angew. Chem.* **1995**, *107*, 232–234; *Angew. Chem. Int. Ed. Engl.* **1995**, *34*, 207–209.
- A search of the CSD (version 5.32, February 2011 update) reveals that only dicarboxy-2,2′-bipyridine ligands have been used to exploit the chelating as well as bridging potential of the 2,2′-bipyridine core, however, none of these structures employs the trischelate moiety.
- a) T. Schareina, C. Schick, B. F. Abrahams, R. Kempe, *Z. Anorg. Allg. Chem.* **2001**, *627*, 1711–1713; b) T. Schareina, C. Schick, R. Kempe, *Z. Anorg. Allg. Chem.* **2001**, *627*, 131–133; c) Y.-H. Liu, Y.-L. Lu, H.-C. Wu, J.-C. Wang, K.-L. Lu, *Inorg. Chem.* **2002**, *41*, 2592–2597; d) E. Tynan, P. Jensen, N. R. Kelly, P. E. Kruger, A. C. Lees, B. Moubarak, K. S. Murray, *Dalton Trans.* **2004**, 3440–3447; e) E. Tynan, P. Jensen, P. E. Kruger, A. C. Lees, *Chem. Commun.* **2004**, 776–777; f) J. Hafizovic, U. Olsbye, K. P. Lillerud, *Acta Crystallogr.*

- Sect. E **2007**, 63, m962–m964; g) N. R. Kelly, S. Goetz, S. R. Batten, P. E. Kruger, *CrystEngComm* **2008**, 10, 68–78; h) C.-Q. Zhang, F. Fu, D.-S. Li, Y.-X. Ren, X.-Z. Zhao, *Synth. React. Inorg. Met.-Org. Nano-Met. Chem.* **2008**, 38, 652–656; i) M. Fang, B. Zhao, Y. Zuo, J. Chen, W. Shi, J. Liang, P. Cheng, *Dalton Trans.* **2009**, 7765–7770; j) C.-C. Wang, *Asian J. Chem.* **2009**, 21, 4711–4720; k) A. J. Blake, N. R. Champness, T. L. Easun, D. R. Allan, H. Nowell, M. W. George, J. Jia, X.-Z. Sun, *Nat. Chem.* **2010**, 2, 688–694; l) J. Z. Gu, Z. Q. Gao, W. Dou, M. Y. Tan, *Chin. J. Struct. Chem.* **2010**, 29, 519–524; m) A. Kobayashi, T. Yonemura, M. Kato, *Eur. J. Inorg. Chem.* **2010**, 2465–2470.
- [9] G. R. Newkome, A. K. Patri, E. Holder, U. S. Schubert, *Eur. J. Org. Chem.* **2004**, 235–254.
- [10] For examples of spontaneous resolution, see: a) B. Gil-Hernández, H. A. Hoeppe, J. K. Vieth, J. Sanchiz, C. Janiak, *Chem. Commun.* **2010**, 46, 8270–8272; b) H. D. Flack, *Acta Crystallogr. Sect. A* **2009**, 65, 371–389; c) C. Janiak, A.-C. Chamayou, A. K. M. R. Uddin, M. Uddin, K. S. Hagen, M. Enamullah, *Dalton Trans.* **2009**, 3698–3709; d) M. Enamullah, A. Sharmin, M. Hasegawa, T. Hoshi, A. C. Chamayou, C. Janiak, *Eur. J. Inorg. Chem.* **2006**, 2146–2154.
- [11] a) Y. Inokuma, T. Arai, M. Fujita, *Nat. Chem.* **2010**, 2, 780–783; b) B. F. Abrahams, S. R. Batten, H. Hamit, B. F. Hoskins, R. Robson, *Angew. Chem.* **1996**, 108, 1794–1796; *Angew. Chem. Int. Ed. Engl.* **1996**, 35, 1690–1692; c) H. M. El-Kaderi, J. R. Hunt, J. L. Mendoza-Cortes, A. P. Cote, R. E. Taylor, M. O’Keeffe, O. M. Yaghi, *Science* **2007**, 316, 268–272; d) S. S. Y. Chui, S. M. F. Lo, J. P. H. Charmant, A. G. Orpen, I. D. Williams, *Science* **1999**, 283, 1148–1150; e) F. Nouar, J. F. Eubank, T. Bousquet, L. Wojtas, M. J. Zaworotko, M. Eddaoudi, *J. Am. Chem. Soc.* **2008**, 130, 1833–1835; f) J. J. Perry IV, J. A. Perma, M. J. Zaworotko, *Chem. Soc. Rev.* **2009**, 38, 1400–1417.
- [12] a) V. A. Blatov, A. P. Shevchenko, V. N. Serezhkin, *J. Appl. Crystallogr.* **2000**, 33, 1193; b) M. O’Keeffe, M. Eddaoudi, H. L. Li, T. Reincke, O. M. Yaghi, *J. Solid State Chem.* **2000**, 152, 3–20.
- [13] a) N. G. Naumov, A. V. Virovets, M. N. Sokolov, S. B. Artemkina, V. E. Fedorov, *Angew. Chem.* **1998**, 110, 2043–2045; *Angew. Chem. Int. Ed.* **1998**, 37, 1943–1945; b) N. G. Naumov, A. V. Virovets, S. B. Artemkina, D. Y. Naumov, J. A. K. Howard, V. E. Fedorov, *J. Solid State Chem.* **2004**, 177, 1896–1904; c) Y. Liu, J. F. Eubank, A. J. Cairns, J. Eckert, V. C. Kravtsov, R. Luebke, M. Eddaoudi, *Angew. Chem.* **2007**, 119, 3342–3347; *Angew. Chem. Int. Ed.* **2007**, 46, 3278–3283.
- [14] a) B. Wu, J. Yang, X. Huang, S. Li, C. Jia, X.-J. Yang, N. Tang, C. Janiak, *Dalton Trans.* **2011**, 40, 5687–5696; b) B. Wu, X. J. Yang, C. Janiak, P. G. Lassahn, *Chem. Commun.* **2003**, 902–903.
- [15] a) Y. Wang, T.-a. Okamura, W.-Y. Sun, N. Ueyama, *Cryst. Growth Des.* **2008**, 8, 802–804; b) R. A. Smaldone, R. S. Forgan, H. Furukawa, J. J. Gassensmith, A. M. Z. Slawin, O. M. Yaghi, J. F. Stoddart, *Angew. Chem.* **2010**, 122, 8812–8816; *Angew. Chem. Int. Ed.* **2010**, 49, 8630–8634; c) K. S. Jeong, Y. B. Go, S. M. Shin, S. J. Lee, J. Kim, O. M. Yaghi, N. Jeong, *Chem. Sci.* **2011**, 2, 877–882; d) L. R. MacGillivray, J. L. Atwood, *Nature* **1997**, 389, 469–472.
- [16] a) J. Pauls, S. Chitsaz, B. Neumuller, *Z. Anorg. Allg. Chem.* **2000**, 626, 2028–2034; b) S. Chitsaz, B. Neumuller, *Organometallics* **2001**, 20, 2338–2343; c) A. J. Amoroso, S. S. M. Chung, D. J. E. Spencer, J. P. Danks, M. W. Glenny, A. J. Blake, P. A. Cooke, C. Wilson, M. Schroder, *Chem. Commun.* **2003**, 2020–2021.
- [17] For examples of heterometallic coordination polymers, see: a) B. Kilduff, D. Pogozhev, S. A. Baudron, M. W. Hosseini, *Inorg. Chem.* **2010**, 49, 11231–11239; b) C. L. Cahill, D. T. de Lill, M. Frisch, *CrystEngComm* **2007**, 9, 15–26; c) S. R. Halper, S. M. Cohen, *Inorg. Chem.* **2005**, 44, 486–488; d) D. W. Ryu, W. R. Lee, J. W. Lee, J. H. Yoon, H. C. Kim, E. K. Koh, C. S. Hong, *Chem. Commun.* **2010**, 46, 8779–8781; e) D. Sun, D.-F. Wang, X.-G. Han, N. Zhang, R.-B. Huang, L.-S. Zheng, *Chem. Commun.* **2011**, 47, 746–748.
- [18] a) M.-D. Serb, M. Speldrich, H. Lueken, U. Englert, *Z. Anorg. Allg. Chem.* **2011**, 637, 536–542; b) B. Jee, K. Eisinger, F. Gul-E-Noor, M. Bertmer, M. Hartmann, D. Himsl, A. Poepl, *J. Phys. Chem. C* **2010**, 114, 16630–16639; c) M. Lusi, J. L. Atwood, L. R. MacGillivray, L. J. Barbour, *CrystEngComm* **2011**, 13, 4311–4313.
- [19] M. Schwalbe, B. Schafer, H. Gorls, S. Rau, S. Tschierlei, M. Schmitt, J. Popp, G. Vaughan, W. Henry, J. G. Vos, *Eur. J. Inorg. Chem.* **2008**, 3310–3319.
- [20] G. M. Sheldrick, *Acta Crystallogr. Sect. A* **2008**, 64, 112–122.
- [21] M. C. Burla, R. Caliendo, M. Camalli, B. Carrozzini, G. L. Cascara, L. De Caro, C. Giacovazzo, G. Polidori, R. Spagna, *J. Appl. Crystallogr.* **2005**, 38, 381–388.
- [22] L. J. Barbour, *J. Supramol. Chem.* **2001**, 1, 189–191.
- [23] Persistence of Vision Raytracer, Version 3.6., Williamstown, Australia, **2004**.
- [24] P. Van der Sluis, A. L. Spek, *Acta Crystallogr. Sect. A* **1990**, 46, 194–201.
- [25] A. L. Spek, *Acta Crystallogr. Sect. D* **2009**, 65, 148–155.
- [26] a) H. D. Flack, *Acta Crystallogr. Sect. A* **1983**, 39, 876–881; b) H. D. Flack, M. Sadki, A. L. Thompson, D. J. Watkin, *Acta Crystallogr. Sect. A* **2011**, 67, 21–34; c) H. D. Flack, G. Bernardinelli, *Chirality* **2008**, 20, 681–690; d) H. D. Flack, G. Bernardinelli, *Acta Crystallogr. Sect. A* **1999**, 55, 908–915.

Received: June 28, 2011  
Published online: December 2, 2011